

VIVA: VLM-Guided Instruction-Based Video Editing with Reward Optimization

Xiaoyan Cong^{1,2,*}, Haotian Yang^{2,†}, Angtian Wang², Yizhi Wang², Yiding Yang², Canyu Zhang²
Chongyang Ma²

¹ Brown University ² Intelligent Creation, ByteDance



Figure 1. Example results generated by VIVA in comparison with Runway Gen-4 Aleph [53]. Our method supports instruction-based video editing with an optional reference image as input (shown as the inset teddy bear in the first row). Runway Gen-4 Aleph over-completes the editing instruction, removing both the hand and the cigarette entirely, and fails to preserve the identity of the teddy bear.

Abstract

Instruction-based video editing aims to modify an input video according to a natural-language instruction while preserving content fidelity and temporal coherence. However, existing diffusion-based approaches are often trained on paired data of simple editing operations, which fundamentally limits their ability to generalize to diverse and complex, real-world instructions. To address this generalization gap, we propose VIVA, a scalable framework for instruction-based video editing that leverages VLM-guided encoding and reward optimization. First, we introduce a VLM-based instructor that encodes the textual instruction, the first frame of the source video, and an optional reference image into visually-grounded instruction representations, providing fine-grained spatial and semantic context for the diffusion transformer backbone. Second, we propose a post-training stage, Edit-GRPO, which adapts Group Relative Policy Optimization to the domain of video editing, directly optimizing the model for instruction-faithful, content-preserving, and aesthetically pleasing edits using relative rewards. Furthermore, we propose a data construction pipeline designed to synthetically generate diverse, high-fidelity paired video–instruction data of basic editing operations. Extensive experiments show that VIVA achieves

superior instruction following, generalization, and editing quality over state-of-the-art methods. Website: <https://viva-paper.github.io/>.

1. Introduction

Video editing plays a central role in modern digital media creation, enabling applications such as film post-production, advertising, and language-guided content personalization [13, 24, 35, 53, 73]. Recent diffusion-based approaches typically formulate video editing as a supervised translation problem from an input video and an editing instruction to an edited output. This formulation relies on carefully constructed paired datasets of source videos and corresponding edited targets or text prompts [8, 13, 14, 25, 73, 75].

However, the practical construction of such paired training data faces a significant bottleneck: existing synthesis pipelines are largely confined to generating pairs for highly simplified editing tasks. These are often limited to basic operations like single object addition, deletion, or object swaps strictly within a predefined mask [8, 10, 73, 75]. It remains extremely difficult to automatically generate training pairs for more general and complex edits, such as combining multiple tasks, performing object swaps outside of the original mask, changing the global environment (e.g., weather or season), or executing other semantically-aware

*Work done while Xiaoyan Cong was an intern at ByteDance.

†Project Lead.

controls.

This reliance on training data comprised of simplistic edits fundamentally limits the generalization capabilities of current video editing systems. When faced with open-domain or complex real-world scenarios, their performance degrades. To address this generalization gap, we introduce a method to improve model performance on complex editing tasks, even when trained only on limited, simple editing pairs. Specifically, we introduce two complementary components that enhance how instructions are represented and how the video editing model is optimized for output quality.

First, we introduce the *VLM instructor*, a vision-language model used as a multimodal instruction encoder. Given the first frame of the input video together with the user’s editing instructions, the VLM produces a sequence of grounded, fine-grained multimodal tokens that jointly encode the target entities, spatial regions, and desired attribute changes. These tokens are then fed as conditioning signals into the diffusion transformer (DiT) backbone, in place of standard text embeddings. Recent large vision-language models demonstrate strong capabilities in aligning visual content with detailed natural-language instructions and conversations [38, 45], and we leverage this capacity to obtain richer, disambiguated instruction representations. This approach allows us to effectively combine the advanced visual-linguistic understanding of the VLM with the high-fidelity video generation capability of the pre-trained DiT.

Second, we introduce *Edit-GRPO*, a post-training stage that explicitly optimizes the model toward successful edits via reinforcement learning (RL). Building on Group Relative Policy Optimization (GRPO) [39, 55], which has been shown to improve reasoning ability in large language models by comparing groups of sampled outputs under task-specific rewards, we adapt the same principle to text-guided video editing. For each input video and carefully designed editing instruction, the model generates multiple candidate edited videos; we then compute edit-specific rewards that measure instruction fidelity, identity preservation, and structural consistency, and use the relative scores within each group to update the policy. This edit-centric RL phase focuses learning on semantic correctness rather than pixel-level reconstruction alone. Previous methods for image editing have employed iterative synthesis, where a model is trained, used to generate new pairs, and then good pairs are labeled and added back to the training set [56]. This process can be formulated as rejection-with-resampling (RWR) [31, 47] in an RL paradigm. In contrast, our approach directly uses an online RL method GRPO, which more effectively extracts supervision from each limited paired example to achieve better editing performance.

Furthermore, we propose a pipeline to construct a high-quality, synthetic dataset. This dataset consists of paired

videos (original and edited) accompanied by accurate text instructions. Our pipeline is designed to generate video pairs demonstrating strict local editing and high fidelity, which cover a diverse range of basic editing operations, providing a solid foundation for training our model.

In summary, our contributions include:

- The VLM instructor that jointly processes the first frame and text to provide visually-grounded instruction representations for the video editor.
- A post-training stage, termed Edit-GRPO, that directly rewards successful, instruction-faithful edits.
- A data construction pipeline that generates diverse, high-quality paired video–instruction dataset of basic editing operations.
- Extensive evaluations showing superior instruction following without degrading video quality compared to strong baselines.

2. Related Work

Instruction-based video editing. Natural language–driven video transformation enables intuitive and controllable edits while maintaining visual fidelity. Earlier methods [8, 11, 16, 19, 26, 30, 33, 42, 48, 63, 68] leveraged inversion-based approaches [57] to perform zero-shot or one-shot text-driven edits on videos. With the advent of open-source pretrained video diffusion models [21, 29, 60], a wave of task-specific solutions emerged for video addition [59, 74], inpainting [5, 76], virtual try-on [17, 27, 77], and character replacement/animation [9]. Although effective in limited scenarios, these approaches typically depend on manual priors such as masks, poses, or motion trajectories, which limit flexibility and generalization. InsV2V [10] pioneers instruction-only video editing by utilizing InstructPix2Pix [6] to synthesize paired video editing data. However, its results were hindered by the limited data quality and backbone performance. More recent efforts [14, 24, 25, 35, 53, 70, 71] have scaled instruction-based editing with notable gains. Ditto [3] supplies a pretrained backbone with a series of trainable context-blocks. Concurrent works like InstructX [46], Omni-Video [58], OmniV2V [34], and Univideo [66] also harness VLM’s understanding capacities to aid video editing, demonstrating impressive progress.

VLMs for visual understanding and generation. Vision–language models (VLMs) provide a bridge between visual perception and textual description. Foundational VLMs such as CLIP [49], BLIP-2 [32], and Flamingo [1] learn joint representations that align visual content with textual descriptions. Instruction-tuned variants, including LLaVA [37], Video-ChatGPT [45], and Qwen2.5-VL [4], further enhance visual grounding and context-aware textual comprehension. These advances show that pretrained

VLMs can serve as powerful priors for conditional control in video generation. Building on this foundation, our work adopts a VLM-based instructor to encode both textual instructions and visual context, improving controllability and instruction fidelity in video editing.

Reinforcement learning for generative models. Reinforcement learning has emerged as an effective approach for enhancing model alignment and controllability. Algorithms such as PPO [54], RPO [51], and GRPO [55] have been widely adopted in large language models to refine instruction-following and preference alignment. Recent studies [39, 40, 65, 69] have extended these ideas to visual generation, while other works [44, 67] focus on image editing, employing reward-guided fine-tuning to better align generative edits with user intent. We extend these approaches for video editing to comprehensively enhance overall performance, robustness, and generalization.

3. Method

As illustrated in Figure 2, VIVA employs a Diffusion Transformer (DiT) [29] as the generation branch and a Vision-Language Model (VLM) instructor as the understanding branch. Section 3.1 describes how the VLM instructor aggregates and interprets diverse multimodal conditions, including a text instruction, a source video, and an optional reference image. Section 3.2 introduces how VIVA adapts and fine-tunes a pretrained text-to-video (T2V) DiT to perform versatile instruction-based video editing using the semantic context provided by the VLM instructor and the source video. To enhance instruction following, content fidelity, and visual aesthetics, we introduce a post-training strategy based on Group Relative Policy Optimization (GRPO), termed *Edit-GRPO*, in Section 3.3. Section 3.4 presents our data preparation process that generates diverse and high-quality video editing dataset.

3.1. Context-Aware VLM Instructor

Since video editing is a highly context-aware task, it is critical and non-trivial to interpret the complicated relationship between diverse multimodal conditions among text instructions, source videos, and optionally provided reference images. We argue that an encoder exposed only to the language space, such as T5 series [50], struggles to provide sufficient semantic guidance, thereby introducing more difficulty and ambiguity to the subsequent generation branch. Instead, VLM achieves more robust alignment between language space and visual feature space, making it inherently a great alternative for understanding and processing multimodal context. There have been several works trying to connect a VLM such as QWen2.5-VL [4] with a DiT pretrained on T5 space such as Wan [60]. However, such strat-

egy requires a heavy pretraining stage for aligning the feature space of the VLM with the generation space of the DiT. Thus, we choose Hunyuan-T2V-13B [29] as our backbone, as its pretrained model has already aligned with the VLM space (llava-llama-3-8b [12]).

Solely relying on an input of semantically sparse textual instructions \mathbf{t}_{ins} often leads to a less underspecified conditioning signal, causing ambiguity for the subsequent editing process. To address this limitation, we propose augmenting the input by incorporating the first frame \mathbf{I}_{src} sampled from the source video \mathbf{V}_{src} . The introduction of \mathbf{I}_{src} significantly enriches the condition tokens with grounded, fine-grained semantic bias. Consequently, the VLM is better equipped to interpret the intricate relationship between the editing instruction and the source video. This integrated understanding allows the VLM to implicitly distinguish critical elements, such as the intended editing region and the specific editing entity. By providing the DiT with such fine-grained and accurate control signals, our approach effectively overcomes the ambiguity caused by the sparse conditioning inherent in instruction-only designs, ultimately yielding higher fidelity and more controllable video editing. To further support a broader range of multimodal control and enhance the user’s flexibility to specify the exact editing outcome, our VLM instructor allows an optional reference image input \mathbf{I}_{ref} . While the editing instruction dictates what transformation should occur, the reference image explicitly grounds how the edited content should look. This additional visual context takes more advantages of VLM’s multimodal understanding and thinking abilities to generate more detailed and accurate editing guidance.

We take the last hidden states from the VLM instructor as our multimodal condition tokens \mathbf{x}_{vlm} :

$$\mathbf{x}_{vlm} = \text{VLM}(\mathbf{t}_{ins}, \mathbf{I}_{src}, \mathbf{I}_{ref}). \quad (1)$$

3.2. Instruction-based Supervised Fine-Tuning

To effectively preserve the multimodal understanding and reasoning capabilities inherent in the VLM, we freeze its parameters throughout the training process, without losing its strong generalization ability. While the pretrained DiT weights of the HunyuanT2V model are already strongly aligned with the VLM’s language space, the introduction of additional visual information \mathbf{I}_{src} and \mathbf{I}_{ref} requires a careful adaptation strategy. In addition to finetuning the DiT, we introduce and train a lightweight Token Refiner \mathcal{R} to enhance the DiT’s comprehensive responsiveness to the visual conditioning signals, as well as the understanding of the underlying connections between textual and visual conditioning information.

To enhance the editing consistency with \mathbf{V}_{src} , we concatenate it with the noise in the channel dimension. Such design intuitively and effectively introduces a spatially and

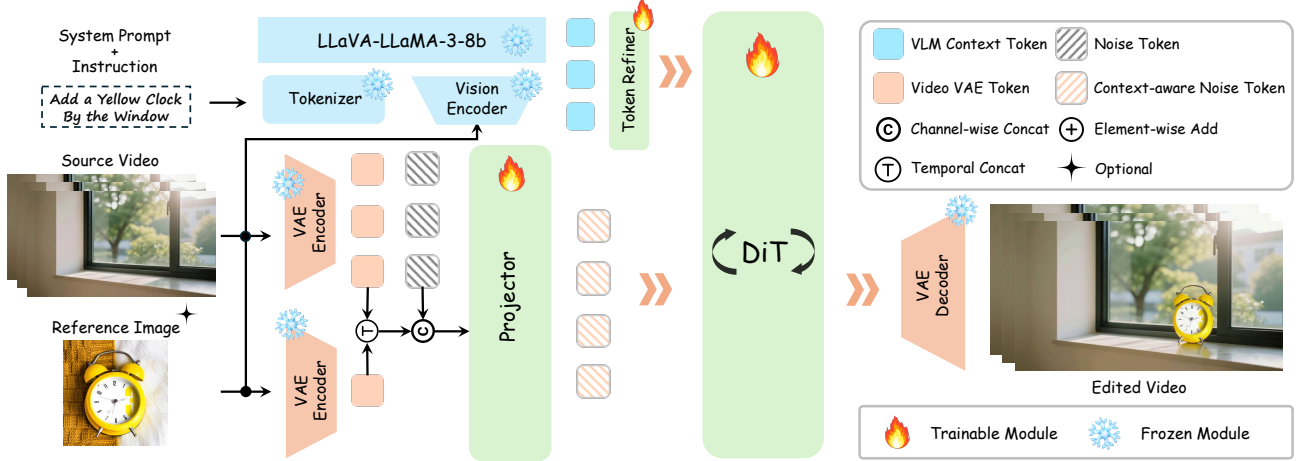


Figure 2. Overall pipeline of VIVA. A context-aware VLM instructor encodes the system prompt, instruction, first frame of the source video, and an optional reference image into VLM tokens. A trainable token refiner aligns these tokens to the pretrained DiT latent space. The VAE encodings of the source video and optional reference image are added to the noisy latent to form context-aware noise tokens. Finally, the DiT denoises these tokens under VLM guidance to generate the edited video.

temporally aligned inductive bias, thereby providing the denoising process with rich and strong contextual guidance of the structure and motion of the source video. Specifically, a VAE latent \mathbf{z}_{src} of \mathbf{V}_{src} and a noise latent \mathbf{z}_{noise} are patchified and unfolded into a 1D sequence of tokens $\mathbf{x}_{src} \in \mathbb{R}^{L \times C}$ and $\mathbf{x}_{noise} \in \mathbb{R}^{L \times C}$ separately. These two sequence of tokens are then channel-concatenated to get $[\mathbf{x}_{src}, \mathbf{x}_{noise}] \in \mathbb{R}^{L \times 2C}$. Then the context-aware noisy video tokens can be formulated as

$$\mathbf{x}_{video} = \mathcal{P}(\text{Concat}(\mathbf{P}(\mathbf{z}_{src}), \mathbf{P}(\mathbf{z}_{noise})))^c, \quad (2)$$

where $\mathbf{x}_{video} \in \mathbb{R}^{L \times C}$, $\text{Concat}(\cdot, \cdot)^c$ represents channel-wise concatenation, \mathbf{P} is a patchification module, and \mathcal{P} indicates a trainable projector that aggregates the contextual video information along the channel dimension to align with the feature dimension of the DiT.

With the multimodal condition tokens \mathbf{x}_{vlm} and context-aware video tokens \mathbf{x}_{video} , we use Flow Matching [36] for model training. In this supervised fine-tuning stage, we train the patchify module \mathbf{P} , the projector \mathcal{P} , the token refiner \mathcal{R} , and the entire DiT on the synthetic paired source/target-video-instruction dataset constructed by ourselves. Due to the inherent scarcity of paired video editing data and the limited range of editing types, we incorporate large-scale image editing data as a supplement through treating an image as a video with one frame. Experiments demonstrate that various editing capabilities within the image domain have effectively been transferred to the video domain, such as global stylization editing, which does not exist in our paired video data.

With the mask video M generated during the data preparation introduced in Section 3.4, we augment the vanilla

Rectified Flow loss into a masked version as:

$$\mathcal{L}_{\text{mask}} = (\mathbf{1} + w_m M) \mathcal{L}_{\text{FM}}, \quad (3)$$

where w_m is the mask weight.

3.3. Edit-GRPO

To further enhance model performance, we design a sophisticated reward system via GRPO, focusing on improving the instruction following ability, source video preservation, and human preference alignment. The overall pipeline of Edit-GRPO is presented in Figure 3.

Instruction following. The accurate and high-quality instruction following ability is the most fundamental metric for evaluating the performance of an instruction-based video editing model. However, since a direct reward model to quantify this does not yet exist, we design the objective as $(C(\mathbf{V}_{edit}, \mathbf{t}_{edit}) - C(\mathbf{V}_{src}, \mathbf{t}_{edit})) + (C(\mathbf{V}_{src}, \mathbf{t}_{src}) - C(\mathbf{V}_{edit}, \mathbf{t}_{src}))$, where \mathbf{t}_{src} is the source video description, \mathbf{t}_{edit} is the paired edited video description, \mathbf{V}_{src} is the source video, \mathbf{V}_{edit} is the edited video, and $C(V, \mathbf{t})$ is the Clip similarity between a video and a description. Intuitively, we want \mathbf{V}_{edit} to be more aligned with \mathbf{t}_{edit} than \mathbf{V}_{src} , and \mathbf{V}_{src} to be more aligned with \mathbf{t}_{src} than \mathbf{V}_{edit} .

Since $C(\mathbf{V}_{src}, \mathbf{t}_{edit})$ and $C(\mathbf{V}_{src}, \mathbf{t}_{src})$ are identical for the samples within the group, they make no contribution to the gradient update due to the nature of group relative preference. The instruction following score can then be formulated as:

$$\mathbf{R}_{\text{IF}} = C(\mathbf{V}_{edit}, \mathbf{t}_{edit}) - C(\mathbf{V}_{edit}, \mathbf{t}_{src}). \quad (4)$$

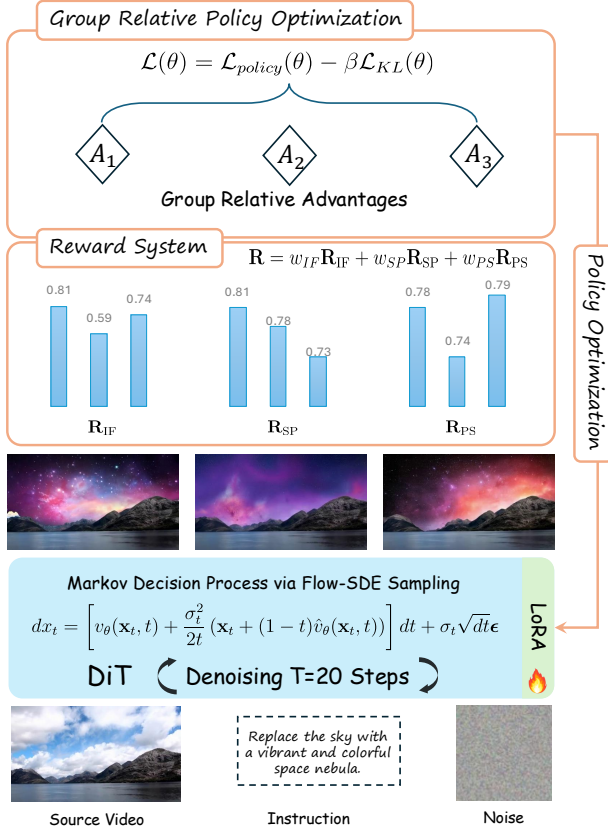


Figure 3. Overall pipeline of Edit-GRPO. We inject stochasticity via Flow-SDE [39] to generate diverse samples, score them with our reward system, and compute a GRPO loss from the resulting relative advantages to update the model. For efficiency, we optimize a LoRA instead of full fine-tuning.

Source video preservation. A further key metric in video editing is that regions outside the edit should preserve high fidelity to the source video, and the edited content must also be coherent with the source video. We thus propose the following objective to quantify source video preservation reward score:

$$\mathbf{R}_{SP} = C(\mathbf{V}_{src}, \mathbf{V}_{edit}). \quad (5)$$

Human preference alignment. To align video editing results with human preferences, we use Pickscore to comprehensively evaluate the alignment of the edited video with the instruction and its visual quality:

$$\mathbf{R}_{PS} = \text{Pickscore}(\mathbf{V}_{edit}, \mathbf{t}_{edit}). \quad (6)$$

Overall, we use a combination of the aforementioned reward scores as the optimization objective to improve the model’s capabilities of instruction following, source video preservation, and the human preference alignment.

$$\mathbf{R} = w_{IF}\mathbf{R}_{IF} + w_{SP}\mathbf{R}_{SP} + w_{PS}\mathbf{R}_{PS}, \quad (7)$$

where w_{IF} , w_{SP} , and w_{PS} are reward balancing weights. Instead of full fine-tuning, we opt to train a LoRA [22] on the DiT backbone during the Edit-GRPO stage for efficiency. Please refer to the supplementary materials for the detailed LoRA design.

3.4. Data Preparation

The field currently lacks a publicly available, large-scale, high-quality dataset of paired video editing examples. Existing datasets [2, 75], which often rely on inpainting or first-frame transfer guided by dense control signals (*e.g.*, depth and edges), frequently suffer from visual artifacts, background inconsistencies, and inaccurate instructional alignment. To address this gap, we construct a large-scale video editing dataset comprising 1.5 million pairs, covering diverse local editing types and corresponding instructions.

Our data generation process begins with a pre-trained text-to-video foundation model. We augment the MMDiT [15] architecture with an additional branch for video input, which is then fine-tuned on a meticulously designed dataset. This fine-tuned model is subsequently used to synthesize the video pairs. Empirically, we find that adding this dedicated branch significantly outperforms the typically-used ControlNet [72]. We build our dataset following the steps described below, with more details available in the supplementary materials.

Object replacement. We first extract the names of main objects from a detailed video caption. Then, we use Grounding-DINO [41] to detect the object on the first frame and employ SAM 2 [52] to track its mask throughout the video. These masked video pairs are used to train a local inpainting model. Subsequently, we use an LLM to analyze the original video caption, rewrite it to reflect a new object, and use this new caption to inpaint the masked video, thereby synthesizing the editing pair.

Object addition and removal. We introduce random masks onto a video and train an inpainting model to fill these regions. To synthesize an editing pair, we alter the original video’s caption to remove the masked object and use this new caption for video inpainting. We also add the name of the masked object to the negative prompt to prevent a similar object from being inpainted in the masked region.

Global content editing. We extract dense scribbles from the source video and train a model to synthesize new videos conditioned on this structural guidance and a modified caption. These modified captions are automatically generated by an LLM, which alters the original description (*e.g.*, changing the background setting from “day” to “night”).

Data filtering. The synthesis process described above is inherently prone to artifacts. Instead of relying on unreliable filtering, we employ a two-stage quality control strat-

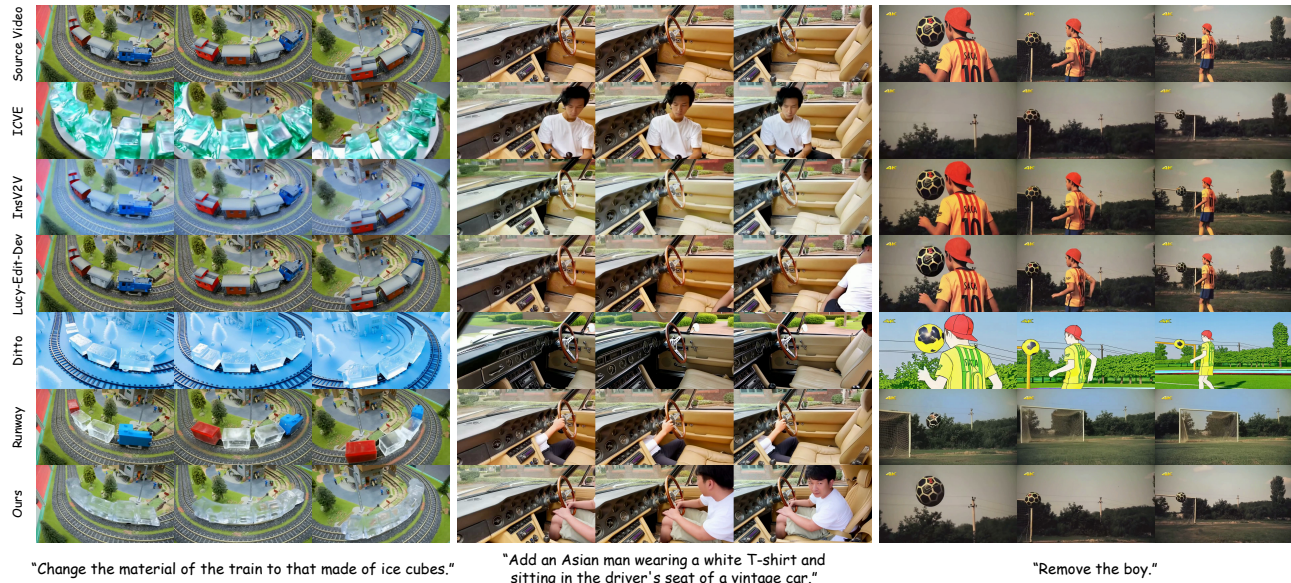


Figure 4. Qualitative comparison of the instruction-based video editing on the VIE-Bench [46] dataset. The editing instruction corresponding to each group of results is shown at the bottom.

egy. First, we use a VLM to rewrite the instructions for the synthesized pairs. Second, we task the VLM with labeling whether the synthesized video is free from artifacts. We primarily use the synthesized video as the source and the real video as the target. We randomly choose a synthesized video as the target only when it is labeled as artifact-free. This setup ensures the editing model is not trained on degraded videos. After testing different VLMs, we select Gemini 2.5 Pro to write the detailed editing instructions.

Image editing pairs. In addition, we collect 5.4 million image editing pairs from publicly available datasets [18, 64]. These image pairs are used to jointly train our editing model by treating each image as a single-frame video. We find that incorporating image data substantially enhances the diversity of editing types that the model can handle.

4. Experiments

4.1. Implementation Details

We use the pretrained *HunyuanVideo-T2V-13B* as the DiT backbone and finetune it on our collected paired training data for 12,000 steps. We set the learning rate to 2×10^{-5} , with a global batch size of 128. To balance the mixing of image and video data, we sample video data with a probability of 0.4 and image data with a probability of 0.6. Please refer to the supplementary materials for details.

4.2. Experimental Setup

Benchmark and baselines. To rigorously evaluate our model’s instruction-based video editing capabilities, we utilize the VIE-Bench benchmark [46], which comprises 140

high-quality instances across diverse instruction-based editing categories, covering both reference-free and reference-based edits. We compare VIVA with five state-of-the-art instruction-based video editing methods, including four open-sourced ones, ICVE [35], Lucy-Edit-Dev [14], Ditto [3], and InsV2V [10], and one commercial model, Runway Gen-4 Aleph [53].

Metrics. Since standard metrics like CLIP-based text-video alignment and PickScore [28] are tailored for target-prompt-based editing evaluation, they are unable and unsuitable to evaluate the performance of instruction adherence. Therefore, following prior works [2, 25, 46], we employ a VLM evaluator (powered by Gemini-2.5-pro) to assign scores (0 – 10) across four critical dimensions: Instruction Following (instruction adherence), Source Preservation (consistency with the source video), Editing Quality (overall video aesthetics), and Subject Similarity (for reference-based edits). As an aiding metric, we also use the VBench [23] evaluation suite to provide quantitative measures of general video quality attributes. We evaluate background consistency and subject consistency by calculating CLIP [49] and DINO [7] feature similarity across frames respectively. Following EditVerse [25], we evaluate the frame-text CLIP [49] feature alignment and video-text ViCLIP [62] feature alignment to reflect both semantics and style consistency. We also evaluate the edited video quality from human preferences perspective by calculating frame-wise PickScore [28].

Category	Task	Method	VLM Evaluation Score					Video Quality				
			Instruction Following	Source Preservation	Editing Quality	Subject Similarity	Avg.	CLIP Consistency	DINO Consistency	Pick-Score	Frame-Text Alignment	Video-Text Alignment
Instruction-only	Add	Runway	9.44	9.16	6.72	-	8.44	97.95	98.39	21.40	28.40	26.30
		ICVE	<u>8.28</u>	<u>8.32</u>	<u>5.08</u>	-	<u>7.22</u>	<u>97.99</u>	<u>98.54</u>	<u>20.53</u>	<u>27.34</u>	<u>25.60</u>
		InsV2V	5.92	5.96	2.80	-	4.89	96.80	97.32	19.88	24.53	21.90
		Lucy-Edit-Dev	6.96	5.40	3.04	-	5.13	97.86	98.40	20.17	25.42	23.38
		Ditto	5.92	7.44	3.72	-	5.69	98.26	98.91	20.51	26.30	24.29
		Ours	9.72	9.80	7.08	-	8.86	97.65	97.70	20.90	27.68	26.32
	Replace	Runway	9.91	9.44	7.79	-	9.04	96.38	96.23	21.18	26.64	26.24
		ICVE	8.20	<u>8.38</u>	<u>4.50</u>	-	<u>7.02</u>	95.95	95.18	<u>20.48</u>	<u>26.06</u>	25.96
		InsV2V	6.17	6.29	3.41	-	5.29	95.14	93.78	20.46	25.15	24.62
		Lucy-Edit-Dev	<u>8.64</u>	6.38	3.23	-	6.08	95.75	94.84	20.39	24.54	24.39
		Ditto	3.70	5.35	3.61	-	4.22	96.78	96.61	20.17	24.26	22.13
		Ours	9.61	9.61	7.35	-	8.86	<u>95.97</u>	<u>95.57</u>	21.03	26.45	<u>25.82</u>
	Remove	Runway	9.86	10.0	9.51	-	9.79	97.62	98.00	20.50	24.35	24.82
		ICVE	<u>7.24</u>	<u>8.68</u>	<u>5.20</u>	-	<u>7.04</u>	97.39	97.40	<u>19.98</u>	<u>22.95</u>	<u>23.30</u>
		InsV2V	5.34	6.72	2.03	-	4.70	95.97	95.70	19.32	21.56	18.76
		Lucy-Edit-Dev	6.65	5.00	3.34	-	5.00	96.58	96.12	19.37	21.10	18.43
		Ditto	4.27	4.27	3.72	-	4.09	<u>97.18</u>	<u>96.99</u>	19.15	20.44	15.63
		Ours	9.37	10.0	8.96	-	9.44	97.17	96.94	20.45	24.36	24.91
	Hybrid Edit	Runway	8.77	8.00	6.77	-	7.85	95.88	95.85	21.50	29.57	30.37
		ICVE	5.55	<u>5.66</u>	<u>3.55</u>	-	<u>4.92</u>	<u>96.01</u>	<u>96.60</u>	20.17	26.70	25.38
InsV2V		4.55	3.44	2.55	-	3.51	94.66	95.27	20.41	<u>27.76</u>	24.93	
Lucy-Edit-Dev		<u>6.66</u>	4.11	3.33	-	4.70	95.50	95.61	<u>20.46</u>	26.31	25.68	
Ditto		2.00	3.11	1.66	-	2.25	96.76	96.88	20.25	26.49	<u>25.88</u>	
Ours		6.88	6.66	4.11	-	5.88	94.99	95.67	20.82	27.87	28.72	
Reference-based	Add	Runway	10.0	10.0	7.20	8.60	8.95	96.22	96.43	20.12	28.36	27.62
		Ours	9.90	10.0	7.00	8.96	8.96	95.92	96.52	19.97	28.11	27.23
	Replace	Runway	9.44	8.22	5.77	8.88	8.07	97.06	97.66	21.37	28.49	29.67
		Ours	9.77	9.88	5.88	9.44	8.74	97.01	97.60	21.20	28.71	30.19

Table 1. Quantitative comparison results on the VIE-Bench [46] dataset. The best and second-best results of the open-sourced methods are highlighted in **bold** and underlined, respectively. As reference-based video editing is not yet supported by the open-source models, we provide our results against the commercial model Runway Gen-4 Aleph [53].

4.3. Qualitative Comparisons

We conduct qualitative comparisons from two perspectives: instruction-only video editing and reference-based video editing, to provide a comprehensive evaluation. Figure 4 presents instruction-only video editing results. We select three representative task examples: local material change (“Change the material of the train to ice cubes.”), subject addition (“Add an Asian man wearing a white T-shirt and sitting in the driver’s seat of a vintage car.”), and subject removal (“Remove the boy.”). In the subject addition example, only our model correctly captures the complex semantics of “sitting in the driver’s seat.” In the material change example, Runway fails to properly interpret the instruction, resulting in incomplete and inaccurate edits, modifying only part of the train. In the removal example, only our model successfully preserves the soccer ball, removes the boy, and maintains background consistency with the source video. These comparisons demonstrate that our model consistently outperforms the baselines, exhibiting superior editing capacity and generalization. We attribute this to our VLM instructor, which supplies the editing backbone with sufficiently rich context, enabling the model to comprehend complex editing semantics and to interpret how these semantics should be applied to the source video.

Since existing open-source instruction-based video edit-

ing models do not support reference-image control, we compare our model only with Runway Gen-4 Aleph. As shown in Figure 1, although Runway responds to the instruction, it fails to accurately align with the reference image. The hat and front label of the teddy bear show noticeable deviations from the reference in the edited results. In contrast, our model correctly understands the intricate relationships among the instruction, the reference image, and the source video, and produces precise editing outcomes. This is enabled by encoding the reference image features into the VLM instructor module, providing ample context to accurately guide our DiT backbone. Please refer to supplementary materials for more results on reference-image controlled video editing.

4.4. Quantitative Comparisons

As shown in Table 1, the quantitative metrics show consistent results with the qualitative comparisons. Our model achieves superior performance over all open-source baselines across all VLM-based evaluations and delivers results on par with the commercial model Runway, demonstrating our model’s strong and robust video editing capability. Since human judgments are more indicative of real-world effectiveness in video editing, we conducted a comprehensive user study with 14 domain experts across three dimen-

Task	Method	VLM Evaluation Score				Video Quality				
		Instruction Following	Source Preservation	Editing Quality	Avg.	CLIP Consistency	DINO Consistency	Pick-Score	Frame-Text Alignment	Video-Text Alignment
Add	Vanilla	6.44	4.56	2.72	4.57	97.49	98.85	19.65	23.38	20.02
	+ V	8.80	7.28	4.52	6.86	98.27	<u>98.63</u>	20.53	26.90	25.28
	+ V + M	<u>8.84</u>	<u>8.68</u>	<u>6.92</u>	<u>8.14</u>	97.33	97.97	20.60	27.38	26.13
	+ V + M + I	8.76	8.32	6.68	7.91	97.56	98.22	21.03	27.90	<u>26.20</u>
	+ V + M + I + E	9.72	9.80	7.08	8.86	<u>97.65</u>	97.70	<u>20.90</u>	<u>27.68</u>	26.32
Replace	Vanilla	4.91	3.70	3.47	4.02	95.63	95.27	19.87	21.33	18.90
	+ V	8.23	6.23	5.05	6.50	96.17	95.07	20.46	24.29	24.06
	+ V + M	7.70	6.91	4.94	6.51	<u>95.79</u>	95.10	20.32	24.47	23.86
	+ V + M + I	9.64	<u>9.50</u>	<u>7.32</u>	<u>8.82</u>	95.73	<u>95.57</u>	<u>20.98</u>	<u>26.44</u>	26.25
	+ V + M + I + E	<u>9.61</u>	9.61	7.35	8.86	95.97	95.57	21.03	26.45	<u>25.82</u>
Remove	Vanilla	2.13	3.75	1.96	2.62	96.44	96.00	18.83	20.49	16.66
	+ V	8.00	8.51	6.44	7.65	97.82	96.77	20.17	23.31	23.38
	+ V + M	8.72	9.06	7.00	8.26	<u>97.35</u>	97.80	20.19	24.19	24.44
	+ V + M + I	<u>9.20</u>	<u>9.82</u>	<u>8.48</u>	<u>9.17</u>	97.30	<u>97.57</u>	<u>20.36</u>	24.44	25.25
	+ V + M + I + E	9.37	10.0	8.96	9.44	97.17	96.94	20.45	<u>24.36</u>	<u>24.91</u>

Table 2. Ablation study results on VIE-Bench. V: VLM instructor; M: masked loss; I: Mixing image data; E: Edit-GRPO. The last row for each task corresponds to our full method. The best and second-best results are highlighted in **bold** and underlined, respectively.

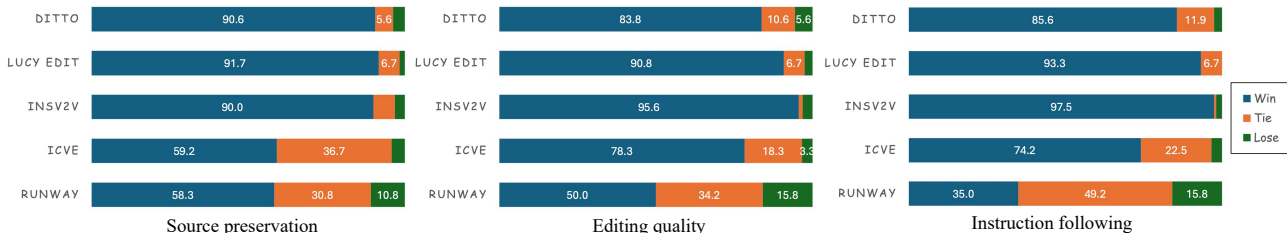


Figure 5. User study results. We conduct 1-to-1 paired comparisons. Win indicates users prefer ours better than baseline, vice versa. Tie indicates there is no significant difference. Numbers are reported in percentage.

sions, following a setup similar to that used in VLM evaluations: (1) Instruction Following: whether the edit precisely follow the editing instruction; (2) Source Preservation: whether the edit maintains coherence with the original video content; (3) Editing Quality: whether the edited video is visually seamless, natural-looking, and pleasing. We randomly sample 30 instruction-only and 10 reference-image-controlled video editing data. Figure 5 quantifies human preference for comparison of generated video from ours versus baselines. Each comparison is labeled as one of three outcomes: G (ours preferred), S (no clear preference / indistinguishable), or B (baseline preferred). Our method is preferred across all three criteria against five baselines.

4.5. Ablation Study

We conduct comprehensive ablations on multiple design choices of our model in Table 2. The introduction of the VLM instructor in Section 3.1 significantly improves performance across all evaluation metrics. It delivers decisive gains in correctly and precisely following editing instructions, demonstrating that feeding visual information into the VLM instructor yields context with rich semantics, which

then better guides the DiT. The masked loss in Eq. 3 introduces an effective spatial inductive bias, enhancing overall editing capability, speeding up convergence, and producing more accurate responses within the edited regions. The strategy of mixing image-editing data during training leverages the larger scale and broader edit-category coverage of image data to significantly improve both editing ability and visual quality. It also enables the emergence of many complex video editing types for which paired video data are typically difficult to obtain. Our full model, with Edit-GRPO, exhibits comprehensive gains in overall editing performance. With the reward system designed in Section 3.3, the model achieves substantial improvements in instruction following, maintaining consistency with the source video. The higher PickScore [28] indicates that the model trained with Edit-GRPO aligns better with human preferences.

5. Conclusion

In this work, we present VIVA, a scalable framework for instruction-based video editing that outperforms existing open-source baselines, achieving state-of-the-art results in

terms of instruction following, edit quality, and generalization. We introduce a VLM-based instructor that encodes both textual instructions and visual inputs into grounded multimodal tokens, substantially improving semantic disambiguation and edit controllability while preserving coherence with the source video. We also propose Edit-GRPO, which, for the first time, adapts Group Relative Policy Optimization to video editing and yields consistent performance gains.

Future work includes expanding the range of supported edit types toward richer and more compositional behaviors, enhancing practical usability by targeting interactive editing, as well as extending to arbitrary resolution and duration. Another promising direction is developing a more general and unified reward model tailored for video editing. Limitations and failure cases are discussed in the supplementary materials.

References

- [1] Jean-Baptiste Alayrac et al. Flamingo: A visual language model for few-shot learning. *arXiv:2204.14198*, 2022. 2
- [2] Qingyan Bai, Qiuyu Wang, Hao Ouyang, Yue Yu, Hanlin Wang, Wen Wang, Ka Leong Cheng, Shuailei Ma, Yanhong Zeng, Zichen Liu, et al. Scaling instruction-based video editing with a high-quality synthetic dataset. *arXiv preprint arXiv:2510.15742*, 2025. 5, 6
- [3] Qingyan Bai et al. Scaling instruction-based video editing with a high-quality synthetic dataset (ditto). *arXiv:2510.15742*, 2025. 2, 6
- [4] Shuai Bai, Keqin Chen, Xuejing Liu, Jialin Wang, Wenbin Ge, Sibao Song, Kai Dang, Peng Wang, Shijie Wang, Jun Tang, et al. Qwen2.5-vl technical report. *arXiv preprint arXiv:2502.13923*, 2025. 2, 3
- [5] Yuxuan Bian, Zhaoyang Zhang, Xuan Ju, Mingdeng Cao, Liangbin Xie, Ying Shan, and Qiang Xu. Videopainter: Any-length video inpainting and editing with plug-and-play context control. In *Proceedings of the Special Interest Group on Computer Graphics and Interactive Techniques Conference Conference Papers*, pages 1–12, 2025. 2
- [6] Tim Brooks, Aleksander Holynski, and Alexei A Efros. Instructpix2pix: Learning to follow image editing instructions. In *Proceedings of the IEEE/CVF conference on computer vision and pattern recognition*, pages 18392–18402, 2023. 2
- [7] Mathilde Caron, Hugo Touvron, Ishan Misra, Hervé Jégou, Julien Mairal, Piotr Bojanowski, and Armand Joulin. Emerging properties in self-supervised vision transformers. In *Proceedings of the IEEE/CVF international conference on computer vision*, pages 9650–9660, 2021. 6
- [8] Yuheng Chen et al. Eve: Efficient zero-shot text-based video editing with diffusion models. In *Proceedings of the International Joint Conference on Artificial Intelligence (IJCAI)*, 2024. 1, 2
- [9] Gang Cheng, Xin Gao, Li Hu, Siqi Hu, Mingyang Huang, Chaonan Ji, Ju Li, Dechao Meng, Jinwei Qi, Penchong Qiao, et al. Wan-animate: Unified character animation and replacement with holistic replication. *arXiv preprint arXiv:2509.14055*, 2025. 2
- [10] Jiaxin Cheng, Tianjun Xiao, and Tong He. Consistent video-to-video transfer using synthetic dataset. In *International Conference on Learning Representations (ICLR)*, 2024. 1, 2, 6
- [11] Yuren Cong, Mengmeng Xu, Christian Simon, Shoufa Chen, Jiawei Ren, Yanping Xie, Juan-Manuel Perez-Rua, Bodo Rosenhahn, Tao Xiang, and Sen He. Flatten: optical flow-guided attention for consistent text-to-video editing. *arXiv preprint arXiv:2310.05922*, 2023. 2
- [12] XTuner Contributors. Xtuner: A toolkit for efficiently fine-tuning llm. <https://github.com/InternLM/xtuner>, 2023. 3
- [13] Paul Couairon, Clément Rambour, Jean-Emmanuel Haugeard, and Nicolas Thome. Videdit: Zero-shot and spatially aware text-driven video editing. In *Advances in Neural Information Processing Systems (NeurIPS)*, 2023. 1
- [14] DecartAI Team. Lucy edit: Open-weight text-guided video editing, 2025. 1, 2, 6
- [15] Patrick Esser, Sumith Kulal, Andreas Blattmann, Rahim Entezari, Jonas Müller, Harry Saini, Yam Levi, Dominik Lorenz, Axel Sauer, Frederic Boesel, et al. Scaling rectified flow transformers for high-resolution image synthesis. In *Forty-first international conference on machine learning*, 2024. 5, 13
- [16] Xiang Fan, Anand Bhattad, and Ranjay Krishna. Videoshop: Localized semantic video editing with noise-extrapolated diffusion inversion. In *European Conference on Computer Vision*, pages 232–250. Springer, 2024. 2
- [17] Zixun Fang, Wei Zhai, Aimin Su, Hongliang Song, Kai Zhu, Mao Wang, Yu Chen, Zhiheng Liu, Yang Cao, and Zheng-Jun Zha. Vivid: Video virtual try-on using diffusion models. *arXiv preprint arXiv:2405.11794*, 2024. 2
- [18] Yuying Ge, Sijie Zhao, Chen Li, Yixiao Ge, and Ying Shan. Seed-data-edit technical report: A hybrid dataset for instructional image editing. *arXiv preprint arXiv:2405.04007*, 2024. 6
- [19] Michal Geyer, Omer Bar-Tal, Shai Bagon, and Tali Dekel. Tokenflow: Consistent diffusion features for consistent video editing. *arXiv:2307.10373*, 2023. 2
- [20] Google. Gemini 2.5: Our most intelligent ai model, 2025. 13, 15
- [21] Wenyi Hong, Ming Ding, Wendi Zheng, Xinghan Liu, and Jie Tang. Cogvideo: Large-scale pretraining for text-to-video generation via transformers. *arXiv preprint arXiv:2205.15868*, 2022. 2
- [22] Edward J Hu, Yelong Shen, Phillip Wallis, Zeyuan Allen-Zhu, Yuanzhi Li, Shean Wang, Lu Wang, Weizhu Chen, et al. Lora: Low-rank adaptation of large language models. *ICLR*, 1(2):3, 2022. 5, 12
- [23] Ziqi Huang, Yinan He, Jiashuo Yu, Fan Zhang, Chenyang Si, Yuming Jiang, Yuanhan Zhang, Tianxing Wu, Qingyang Jin, Nattapol Chanpaisit, et al. Vbench: Comprehensive benchmark suite for video generative models. In *Proceedings of the IEEE/CVF Conference on Computer Vision and Pattern Recognition*, pages 21807–21818, 2024. 6

- [24] Zhaoyang Jiang, Wenqi Zhu, Ming Ding, and et al. Vace: All-in-one video creation and editing. In *ICCV*, 2025. 1, 2
- [25] Xuan Ju, Tianyu Wang, Yuqian Zhou, He Zhang, Qing Liu, Nanxuan Zhao, Zhifei Zhang, Yijun Li, Yuanhao Cai, Shaoteng Liu, et al. Editverse: Unifying image and video editing and generation with in-context learning. *arXiv preprint arXiv:2509.20360*, 2025. 1, 2, 6
- [26] Ozgur Kara, Bariscan Kurtkaya, Hidir Yesiltepe, James M. Rehg, and Pinar Yanardag. Rave: Randomized noise shuffling for fast and consistent video editing with diffusion models. In *Proceedings of the IEEE/CVF Conference on Computer Vision and Pattern Recognition*, 2024. 2
- [27] Johanna Karras, Yingwei Li, Nan Liu, Luyang Zhu, Innfarn Yoo, Andreas Lugmayr, Chris Lee, and Ira Kemelmacher-Shlizerman. Fashion-vidm: Video diffusion model for virtual try-on. In *Proceedings of ACM SIGGRAPH Asia 2024*, 2024. 2
- [28] Yuval Kirstain, Adam Polyak, Uriel Singer, Shahbuland Matiana, Joe Penna, and Omer Levy. Pick-a-pic: An open dataset of user preferences for text-to-image generation. *Advances in neural information processing systems*, 36:36652–36663, 2023. 6, 8
- [29] Weijie Kong, Qi Tian, Zijian Zhang, Rox Min, Zuozhuo Dai, Jin Zhou, Jiangfeng Xiong, Xin Li, Bo Wu, Jianwei Zhang, Kathrina Wu, Qin Lin, Junkun Yuan, Yanxin Long, Aladdin Wang, Andong Wang, Changlin Li, Duojuan Huang, Fang Yang, Hao Tan, Hongmei Wang, Jacob Song, Jiawang Bai, Jianbing Wu, Jinbao Xue, Joey Wang, Kai Wang, Mengyang Liu, Pengyu Li, Shuai Li, Weiyang Wang, Wenqing Yu, Xincheng Deng, Yang Li, Yi Chen, Yutao Cui, Yuanbo Peng, Zhentao Yu, Zhiyu He, Zhiyong Xu, Zixiang Zhou, Zunnan Xu, Yangyu Tao, Qinglin Lu, Songtao Liu, Dax Zhou, Hongfa Wang, Yong Yang, Di Wang, Yuhong Liu, Jie Jiang, and Caesar Zhong. Hunyuanvideo: A systematic framework for large video generative models, 2025. 2, 3, 12
- [30] Max Ku, Cong Wei, Weiming Ren, Harry Yang, and Wenhui Chen. Anyv2v: A tuning-free framework for any video-to-video editing tasks. *arXiv preprint arXiv:2403.14468*, 2024. 2
- [31] Kimin Lee, Hao Liu, Moonkyung Ryu, Olivia Watkins, Yuqing Du, Craig Boutilier, Pieter Abbeel, Mohammad Ghavamzadeh, and Shixiang Shane Gu. Aligning text-to-image models using human feedback. *arXiv preprint arXiv:2302.12192*, 2023. 2
- [32] Junnan Li, Dongxu Li, Silvio Savarese, and Steven Hoi. Blip-2: Bootstrapping language-image pre-training with frozen image encoders and large language models. *arXiv:2301.12597*, 2023. 2
- [33] Xirui Li, Chao Ma, Xiaokang Yang, and Ming-Hsuan Yang. Vidtope: Video token merging for zero-shot video editing. In *Proceedings of the IEEE/CVF Conference on Computer Vision and Pattern Recognition*, pages 7486–7495, 2024. 2
- [34] Sen Liang, Zhentao Yu, Zhengguang Zhou, Teng Hu, Hongmei Wang, Yi Chen, Qin Lin, Yuan Zhou, Xin Li, Qinglin Lu, et al. Omniv2v: Versatile video generation and editing via dynamic content manipulation. *arXiv preprint arXiv:2506.01801*, 2025. 2
- [35] Xinyao Liao, Xianfang Zeng, Ziyi Song, Zhoujie Fu, Gang Yu, and Guosheng Lin. In-context learning with unpaired clips for instruction-based video editing. *arXiv preprint arXiv:2510.14648*, 2025. 1, 2, 6
- [36] Yaron Lipman, Ricky TQ Chen, Heli Ben-Hamu, Maximilian Nickel, and Matt Le. Flow matching for generative modeling. *arXiv preprint arXiv:2210.02747*, 2022. 4, 12
- [37] Haotian Liu, Chunyuan Li, Qingyang Wu, and et al. Visual instruction tuning. In *NeurIPS*, 2023. 2
- [38] Haotian Liu, Chunyuan Li, Qingyang Wu, and Yong Jae Lee. Visual instruction tuning. In *Advances in Neural Information Processing Systems*, 2023. 2
- [39] Jie Liu, Gongye Liu, Jiajun Liang, Yangguang Li, Jiaheng Liu, Xintao Wang, Pengfei Wan, Di Zhang, and Wanli Ouyang. Flow-grpo: Training flow matching models via online rl. *arXiv preprint arXiv:2505.05470*, 2025. 2, 3, 5, 12
- [40] Jie Liu, Gongye Liu, Jiajun Liang, Ziyang Yuan, Xiaokun Liu, Mingwu Zheng, Xiele Wu, Qiulin Wang, Menghan Xia, Xintao Wang, et al. Improving video generation with human feedback. *arXiv preprint arXiv:2501.13918*, 2025. 3
- [41] Shilong Liu, Zhaoyang Zeng, Tianhe Ren, Feng Li, Hao Zhang, Jie Yang, Chunyuan Li, Jianwei Yang, Hang Su, Jun Zhu, et al. Grounding dino: Marrying dino with grounded pre-training for open-set object detection. *arXiv preprint arXiv:2303.05499*, 2023. 5
- [42] Shaoteng Liu, Yuechen Zhang, Wenbo Li, Zhe Lin, and Jiaya Jia. Video-p2p: Video editing with cross-attention control. In *Proceedings of the IEEE/CVF Conference on Computer Vision and Pattern Recognition*, pages 8599–8608, 2024. 2
- [43] Xingchao Liu, Chengyue Gong, and Qiang Liu. Flow straight and fast: Learning to generate and transfer data with rectified flow. *arXiv preprint arXiv:2209.03003*, 2022. 12
- [44] Xin Luo, Jiahao Wang, Chenyuan Wu, Shitao Xiao, Xiyan Jiang, Defu Lian, Jiajun Zhang, Dong Liu, et al. Editscore: Unlocking online rl for image editing via high-fidelity reward modeling. *arXiv preprint arXiv:2509.23909*, 2025. 3
- [45] Muhammad Maaz, Hanoona Rasheed, Salman Khan, and Fahad Khan. Video-ChatGPT: Towards detailed video understanding via large vision and language models. In *Proceedings of the 62nd Annual Meeting of the Association for Computational Linguistics (Volume 1: Long Papers)*, 2024. 2
- [46] Chong Mou, Qichao Sun, Yanze Wu, Pengze Zhang, Xinghui Li, Fulong Ye, Songtao Zhao, and Qian He. Instructxt: Towards unified visual editing with mllm guidance. *arXiv preprint arXiv:2510.08485*, 2025. 2, 6, 7, 13, 15
- [47] Xue Bin Peng, Aviral Kumar, Grace Zhang, and Sergey Levine. Advantage-weighted regression: Simple and scalable off-policy reinforcement learning. *arXiv preprint arXiv:1910.00177*, 2019. 2
- [48] Chenyang Qi, Xiaodong Cun, Yong Zhang, Chenyang Lei, Xintao Wang, Ying Shan, and Qifeng Chen. Fatezero: Fusing attentions for zero-shot text-based video editing. In *Proceedings of the IEEE/CVF International Conference on Computer Vision (ICCV)*, 2023. 2
- [49] Alec Radford, Jong Wook Kim, Chris Hallacy, and et al. Learning transferable visual models from natural language supervision. In *ICML*, 2021. 2, 6

- [50] Colin Raffel, Noam Shazeer, Adam Roberts, Katherine Lee, Sharan Narang, Michael Matena, Yanqi Zhou, Wei Li, and Peter J Liu. Exploring the limits of transfer learning with a unified text-to-text transformer. *Journal of machine learning research*, 21(140):1–67, 2020. 3
- [51] Md Masudur Rahman and Yexiang Xue. Robust policy optimization in deep reinforcement learning. *arXiv preprint arXiv:2212.07536*, 2022. 3
- [52] Nikhila Ravi, Valentin Gabeur, Yuan-Ting Hu, Ronghang Hu, Chaitanya Ryali, Tengyu Ma, Haitham Khedr, Roman Rädle, Chloe Rolland, Laura Gustafson, et al. Sam 2: Segment anything in images and videos. *arXiv preprint arXiv:2408.00714*, 2024. 5
- [53] Runway. Introducing runway aleph, 2025. 1, 2, 6, 7
- [54] John Schulman, Filip Wolski, Prafulla Dhariwal, Alec Radford, and Oleg Klimov. Proximal policy optimization algorithms. *arXiv preprint arXiv:1707.06347*, 2017. 3, 12
- [55] Zihan Shao, Tianyang Cai, Yichang Zhou, et al. DeepSeek-Math: Pushing the limits of mathematical reasoning in open language models. *arXiv preprint arXiv:2402.03300*, 2024. 2, 3, 12
- [56] Yichun Shi, Peng Wang, and Weilin Huang. Seedit: Align image re-generation to image editing. *arXiv preprint arXiv:2411.06686*, 2024. 2
- [57] Jiaming Song, Chenlin Meng, and Stefano Ermon. Denoising diffusion implicit models. *arXiv preprint arXiv:2010.02502*, 2020. 2
- [58] Zhiyu Tan, Hao Yang, Luozheng Qin, Jia Gong, Mengping Yang, and Hao Li. Omni-video: Democratizing unified video understanding and generation. *arXiv preprint arXiv:2507.06119*, 2025. 2
- [59] Yuanpeng Tu, Hao Luo, Xi Chen, Sihui Ji, Xiang Bai, and Hengshuang Zhao. Videoanydoor: High-fidelity video object insertion with precise motion control. In *Proceedings of the Special Interest Group on Computer Graphics and Interactive Techniques Conference Conference Papers*, pages 1–11, 2025. 2
- [60] Team Wan, Ang Wang, Baole Ai, Bin Wen, Chaojie Mao, Chen-Wei Xie, Di Chen, Fei Wu Yu, Haiming Zhao, Jianxia Yang, et al. Wan: Open and advanced large-scale video generative models. *arXiv preprint arXiv:2503.20314*, 2025. 2, 3
- [61] Feng Wang and Zihao Yu. Coefficients-preserving sampling for reinforcement learning with flow matching. *arXiv preprint arXiv:2509.05952*, 2025. 12
- [62] Yi Wang, Yinan He, Yizhuo Li, Kunchang Li, Jiashuo Yu, Xin Ma, Xinhao Li, Guo Chen, Xinyuan Chen, Yaohui Wang, et al. Internvid: A large-scale video-text dataset for multimodal understanding and generation. *arXiv preprint arXiv:2307.06942*, 2023. 6
- [63] Yukun Wang, Longguang Wang, Zhiyuan Ma, Qibin Hu, Kai Xu, and Yulan Guo. Videodirector: Precise video editing via text-to-video models. In *Proceedings of the Computer Vision and Pattern Recognition Conference*, pages 2589–2598, 2025. 2
- [64] Yuhan Wang, Siwei Yang, Bingchen Zhao, Letian Zhang, Qing Liu, Yuyin Zhou, and Cihang Xie. Gpt-image-edit-1.5 m: A million-scale, gpt-generated image dataset. *arXiv preprint arXiv:2507.21033*, 2025. 6
- [65] Yibin Wang, Yuhang Zang, Hao Li, Cheng Jin, and Jiaqi Wang. Unified reward model for multimodal understanding and generation. *arXiv preprint arXiv:2503.05236*, 2025. 3
- [66] Cong Wei, Quande Liu, Zixuan Ye, Qiulin Wang, Xintao Wang, Pengfei Wan, Kun Gai, and Wenhua Chen. Univideo: Unified understanding, generation, and editing for videos. *arXiv preprint arXiv:2510.08377*, 2025. 2
- [67] Jie Wu, Yu Gao, Zilyu Ye, Ming Li, Liang Li, Hanzhong Guo, Jie Liu, Zeyue Xue, Xiaoxia Hou, Wei Liu, et al. Rewarddance: Reward scaling in visual generation. *arXiv preprint arXiv:2509.08826*, 2025. 3
- [68] Jay Zhangjie Wu, Yixiao Ge, Xintao Wang, Stan Weixian Lei, Yuchao Gu, Yufei Shi, Wynne Hsu, Ying Shan, Xiaohu Qie, and Mike Zheng Shou. Tune-a-video: One-shot tuning of image diffusion models for text-to-video generation. In *Proceedings of the IEEE/CVF International Conference on Computer Vision*, pages 7623–7633, 2023. 2
- [69] Zeyue Xue, Jie Wu, Yu Gao, Fangyuan Kong, Lingting Zhu, Mengzhao Chen, Zhiheng Liu, Wei Liu, Qiushan Guo, Weilin Huang, et al. Dancegrpo: Unleashing grpo on visual generation. *arXiv preprint arXiv:2505.07818*, 2025. 3
- [70] Zixuan Ye, Xuanhua He, Quande Liu, Qiulin Wang, Xintao Wang, Pengfei Wan, Di Zhang, Kun Gai, Qifeng Chen, and Wenhua Luo. Unic: Unified in-context video editing. *arXiv preprint arXiv:2506.04216*, 2025. 2
- [71] Siyuan Yu et al. Veggie: Instructional editing and reasoning video concepts with grounded generation. In *ICCV*, 2025. 2
- [72] Lvmin Zhang, Anyi Rao, and Maneesh Agrawala. Adding conditional control to text-to-image diffusion models. In *Proceedings of the IEEE/CVF international conference on computer vision*, pages 3836–3847, 2023. 5
- [73] Min Zhao, Rongzhen Wang, Fan Bao, Chongxuan Li, and Jun Zhu. Controlvideo: Conditional control for one-shot text-driven video editing and beyond. *arXiv preprint arXiv:2305.17098*, 2023. 1
- [74] Shaobin Zhuang, Zhipeng Huang, Binxin Yang, Ying Zhang, Fangyikang Wang, Canmiao Fu, Chong Sun, Zheng-Jun Zha, Chen Li, and Yali Wang. Get in video: Add anything you want to the video. *arXiv preprint arXiv:2503.06268*, 2025. 2
- [75] Bojia Zi, Penghui Ruan, Marco Chen, Xianbiao Qi, Shaozhe Hao, Shihao Zhao, Youze Huang, Bin Liang, Rong Xiao, and Kam-Fai Wong. Se^vnorita-2m: A high-quality instruction-based dataset for general video editing by video specialists. *arXiv preprint arXiv:2502.06734*, 2025. 1, 5
- [76] Bojia Zi, Shihao Zhao, Xianbiao Qi, Jianan Wang, Yukai Shi, Qianyu Chen, Bin Liang, Rong Xiao, Kam-Fai Wong, and Lei Zhang. Cococo: Improving text-guided video inpainting for better consistency, controllability and compatibility. In *Proceedings of the AAAI Conference on Artificial Intelligence*, pages 11067–11076, 2025. 2
- [77] Tongchun Zuo, Zaiyu Huang, Shuliang Ning, Ente Lin, Chao Liang, Zerong Zheng, Jianwen Jiang, Yuan Zhang, Mingyuan Gao, and Xin Dong. Dreamvvt: Mastering realistic video virtual try-on in the wild via a stage-wise diffusion transformer framework. *arXiv preprint arXiv:2508.02807*, 2025. 2

VIVA: VLM-Guided Instruction-Based Video Editing with Reward Optimization

Supplementary Material

A. Preliminaries

A.1. DiT-Based Video Generation and Editing

Diffusion Transformers (DiTs) have become a powerful backbone for modern video generation. They model a sequence of latent video tokens through a transformer-based denoising process conditioned on multimodal inputs such as text or reference frames. DiTs are commonly trained with the *Flow Matching* objective [36], which learns a velocity field $\mathbf{v}_\theta(\mathbf{x}, t)$ that transports a simple prior $p_0(\mathbf{x})$ (e.g., Gaussian noise) toward a target data distribution $p_1(\mathbf{x})$ via a probability flow Ordinary Differential Equation (ODE):

$$\frac{d\mathbf{x}_t}{dt} = \mathbf{v}_\theta(\mathbf{x}_t, t), \quad \text{with } \mathbf{x}_0 \sim p_0(\mathbf{x}). \quad (8)$$

In the commonly used *Rectified Flow* formulation [43], the trajectory is defined as a linear interpolation between noise and data samples:

$$\mathbf{x}_t = (1-t)\mathbf{x}_0 + t\mathbf{x}_1, \quad \mathbf{x}_1 \sim p_1(\mathbf{x}), \quad (9)$$

and the model is trained to regress the target velocity field $\mathbf{u}_t(\mathbf{x}_t) = \frac{d\mathbf{x}_t}{dt} = \mathbf{x}_1 - \mathbf{x}_0$ via the loss:

$$\mathcal{L}_{\text{FM}} = \mathbb{E}_{t, \mathbf{x}_0, \mathbf{x}_1} [\|\mathbf{v}_\theta(\mathbf{x}_t, t) - (\mathbf{x}_1 - \mathbf{x}_0)\|_2^2]. \quad (10)$$

This objective learns a continuous flow that transports noisy latents toward clean samples, providing smoother temporal dynamics and faster convergence than conventional noise-prediction objectives.

For video editing, the DiT backbone is conditioned on the source video and an editing instruction, enabling it to synthesize instruction-aligned output based on the input video.

A.2. Group Relative Policy Optimization (GRPO)

Group Relative Policy Optimization (GRPO) [55] is a recent reinforcement learning algorithm that extends Proximal Policy Optimization (PPO) [54] for efficient post-training alignment. For each input query c , a group of G sampled trajectories $\{\mathbf{x}_t^i\}_{i=1, \dots, G}^{t=0, \dots, T}$ are generated and evaluated by the task-specific reward criterion to get the corresponding reward signals $\{R(\mathbf{x}_0^i)\}_{i=0}^G$. These reward signals are then transformed to relative advantages within the group by:

$$\hat{A}_t^i = \frac{R(\mathbf{x}_0^i) - \text{mean}(\{R(\mathbf{x}_0^i)\}_{i=1}^G)}{\text{std}(\{R(\mathbf{x}_0^i)\}_{i=1}^G)}. \quad (11)$$

This relative formulation reduces variance and stabilizes optimization, making GRPO effective for aligning large generative models with human or semantic preferences.

The policy model is then optimized by maximizing the following objective without requiring a separate critic network:

$$\begin{aligned} \mathcal{L}(\theta) &= \mathbb{E}_{c, \{\mathbf{x}^i\}_{i=1}^G \sim \pi_{\theta, \text{old}}(\cdot|c)} f(r, \hat{A}, \theta, \epsilon, \beta) \\ &= \frac{1}{G} \sum_{i=1}^G \frac{1}{T} \sum_{t=0}^{T-1} (\mathcal{L}_{\text{policy}}(\theta) - \beta \mathcal{L}_{\text{KL}}(\theta)), \end{aligned} \quad (12)$$

where

$$\begin{aligned} \mathcal{L}_{\text{policy}}(\theta) &= \min(r_t^i(\theta) \hat{A}_t^i, \text{clip}(r_t^i(\theta), 1 - \epsilon, 1 + \epsilon) \hat{A}_t^i), \\ \mathcal{L}_{\text{KL}}(\theta) &= D_{\text{KL}}(\pi_\theta \| \pi_{\text{ref}}), \\ r_t^i(\theta) &= \frac{p_\theta(\mathbf{x}_{t-1}^i | \mathbf{x}_t^i, \mathbf{c})}{p_{\theta, \text{old}}(\mathbf{x}_{t-1}^i | \mathbf{x}_t^i, \mathbf{c})}. \end{aligned} \quad (13)$$

Since GRPO relies on stochastic sampling diverse trajectories $\{\mathbf{x}_t^i\}_{i=1, \dots, G}^{t=0, \dots, T}$, Flow-GRPO [39] introduce randomness into Flow Matching by converting the deterministic Flow-ODE into an equivalent Flow-SDE

$$dx_t = \left[v_\theta(\mathbf{x}_t, t) + \frac{\sigma_t^2}{2t} (\mathbf{x}_t + (1-t)\hat{v}_\theta(\mathbf{x}_t, t)) \right] dt + \sigma_t \sqrt{dt} \epsilon \quad (14)$$

where $\epsilon \sim \mathcal{N}(0, I)$ is a newly sampled gaussian noise, $\sigma_t = \eta \sqrt{\frac{t}{1-t}}$ for Flow-GRPO.

Coefficients-Preserving Sampling [61] investigates the problem of an excess of noise injected during Flow-SDE sampling in Eq. 14 and reformulates the sampling process to eliminate the noise artifacts by modifying $\sigma_t = \sin(\frac{\eta\pi}{2})dt$.

B. Implementation Details

During Edit-GRPO, We insert Low-Rank Adaptation (LoRA) [22] modules into the self-attention and cross-attention layers of the DiT [29]. We freeze the parameters of the model after supervised fine-tuning. Only the LoRA parameters are updated, facilitating efficient optimization. For the LoRA configuration, we set the low-rank dimension to $r = 64$ and the scaling factor to $\alpha = 128$. The adapter weights are initialized using a Gaussian distribution.

During inference, we use a classifier-free guidance scale of 2.0, applying it only to instruction conditions. The inference timestep is set to 50 for the balance of performance and inference speed.

C. Data Strategy

C.1. Detailed Architecture for Data Preparation

Having briefly outlined the pipeline for constructing editing pairs in the main text, we now provide the detailed network

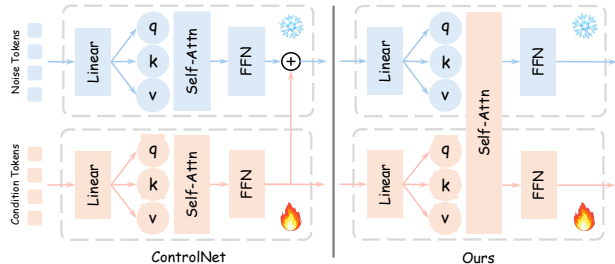


Figure 6. Network architecture for paired data synthesis. We modify the pretrained MMDiT backbone by inserting an additional control branch every four blocks. By concatenating the condition tokens with the noisy latent, the model performs full mutual attention across the sequence, ensuring robust structural alignment between the control signal and the generated video.

architecture used for data synthesis. As illustrated in Figure 6, we integrate an additional branch into the MMDiT architecture [15] to model the interaction between the VAE embeddings of the conditions (e.g., masked video or scribbles) and the noisy latent. The condition tokens and the noisy latent tokens are concatenated, enabling full mutual attention across the entire combined sequence. Furthermore, we align the Rotary Positional Embeddings (RoPE) of the condition tokens with those of the noisy latent tokens. This design is based on the assumption that spatially and temporally corresponding positions in the condition inputs and the target videos are highly correlated and should thus exhibit the highest attention values.

To reduce computational complexity, we insert this additional branch block once every four blocks within the pretrained DiT. During training, we only update the parameters of this additional branch while keeping the pretrained DiT weights frozen to preserve the generative capabilities of the foundation model.

Empirically, we observe that the standard ControlNet architecture is highly sensitive to the Classifier-Free Guidance (CFG) scale. It often generates oversaturated samples at high CFG values, while suffering from poor instruction following at low CFG values. In contrast, our model remains free from saturation artifacts across a wide range of CFG values. We attribute this improvement to the bi-directional attention mechanism between the conditional input and the noisy latent enabled by our branch. Figure 7 visualizes representative training samples spanning addition, removal, replacement, and stylization tasks.

C.2. Edit-GRPO Data

For the Edit-GRPO training stage, only the source videos \mathbf{V}_{src} are required. We curate a subset of high-quality videos and employ Gemini 2.5 Pro [20] to generate suitable editing instructions \mathbf{t}_{ins} for each source video. These prompts are specifically designed to encompass complex combina-

tions of various editing types. We leverage Gemini 2.5 Pro to caption the source video to get the source video prompt \mathbf{t}_{src} . Subsequently, conditioned on \mathbf{t}_{src} and \mathbf{t}_{ins} , Gemini 2.5 Pro generates the target video caption \mathbf{t}_{edit} . This pipeline yields the triplet $(\mathbf{V}_{src}, \mathbf{t}_{src}, \mathbf{t}_{edit})$ required for training Edit-GRPO.

D. Experiments

D.1. Qualitative Comparisons

Figure 8 presents qualitative comparisons of the reference-based video editing on the VIE-Bench [46]. Since existing open-source instruction-based video editing models do not support reference-image control, we compare our model only with Runway Gen-4 Aleph. As shown in Figure 8, although Runway responds to the instruction, it fails to accurately align with the reference image. For example, the toy car and red backpack show noticeable deviations from the reference in the edited results. In contrast, our model correctly understands the intricate relationships among the instruction, the reference image, and the source video, and produces precise editing outcomes.

D.2. Ablation Study on Edit-GRPO

Figure 10 presents qualitative comparisons on before and after applying Edit-GRPO. Edit-GRPO yields a substantial qualitative improvement, consistent with quantitative ablation results in the main paper. In challenging prompts such as “Add a woman with long black hair Lying in the bucket of a green agricultural loader.” and “Replace the man into a gorilla.”, Edit-GRPO preserves the structural integrity and plausibility of the subjects, whereas removing it tends to produce distorted artifacts and collapsing results. For instances like “Add a dinosaur standing on the ground of gas station.” and “Add a big white kitten in the car trunk.”, Edit-GRPO makes the edited areas more natural and realistic, showing exceptional consistency with the source video. Overall, the model equipped with Edit-GRPO demonstrates stronger instruction adherence, higher aesthetic fidelity, more consistent with the source video, and better alignment with human preference.

D.3. Complex Tasks

Figures 11, 12, and 13 present more results of our method on complex instructions that are non-trivial and challenging to be synthesized by the data construction pipeline. Our model is capable of performing complex hybrid instructions like “Make the mountain in the background an active volcano erupting with smoke and lava, and add a little cat running by the couple.”, and non-rigid visual effects such as flames, smokes, fireworks, stylization, and watermark removal. Notably, our model effectively addresses a challenging case in global background editing: ensuring physical

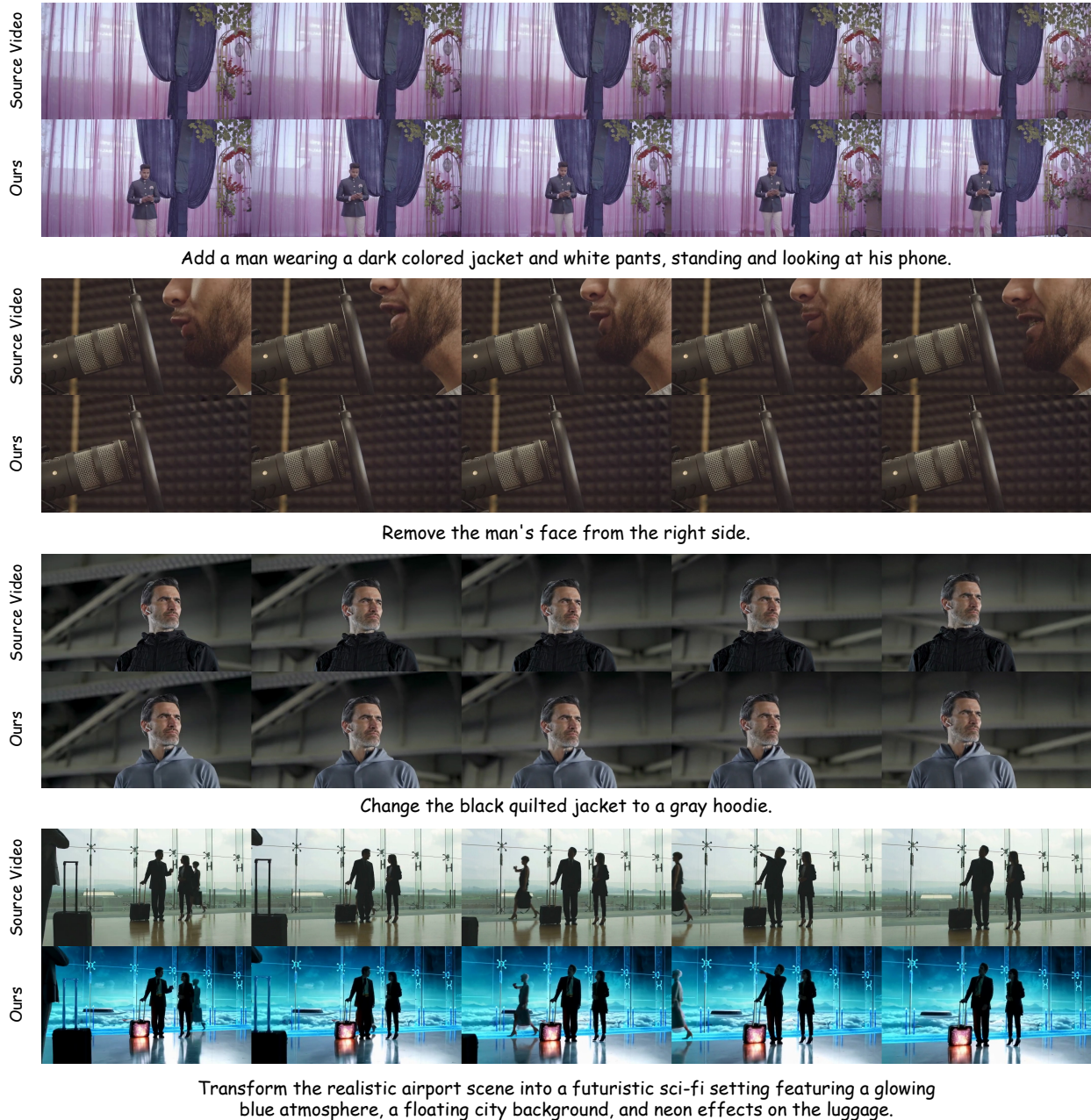


Figure 7. We visualize representative training samples spanning addition, removal, replacement, and stylization tasks, arranged from top to bottom.

coherence between the foreground subject and the edited new environment. This is vividly demonstrated in the example “Change the background from the ocean to a vast, snowy mountain range.” In this scenario, our model successfully synthesizes realistic shadows cast by the subject onto the snowy terrain, thereby achieving a high degree of photorealism and subject-background harmony. Since these complex editing scenarios are difficult to synthesize through the data construction pipeline, they serve as a rigorous test

of a model’s generalization capabilities. We attribute our model’s success to two key factors: First, our VLM instructor possesses an exceptional capacity to interpret the intricate correlation between textual instructions and visual contexts. Second, our strategy of mixing image editing data during training effectively transfers the robust generalization inherent in the image domain to the video editing domain.



Figure 8. Qualitative comparison of the reference-based video editing on the VIE-Bench [46]. The editing instruction is shown at the top and the reference image is shown on the left for each group of results.

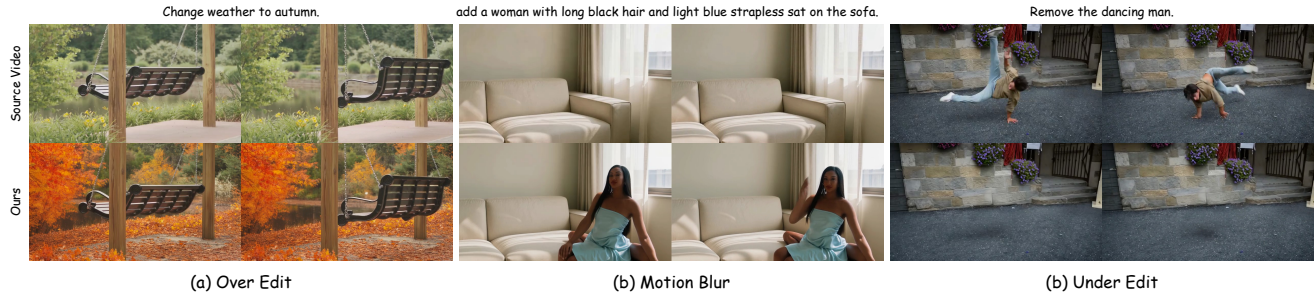


Figure 9. Failure cases. (a) Global transformations such as changing weather sometimes cause over-editing. (a) Rapid motion might occasionally lead to blurry results, such as the woman’s hand. (c) Under-editing might be observed in removal tasks, where residual artifacts, such as cast shadows, remain.

D.4. VLM Evaluation

We employ Gemini-2.5-Pro [20] as the VLM evaluator. Figure 14 presents our VLM evaluation templates for the instruction-based video editing and reference-instruction-based video editing. The VLM evaluator offers a scalable, human-aligned assessment. It is provided with the source frame, the edited frame, the instruction and an optional reference image as inputs, and evaluates the editing perfor-

mance on a scale of 0 (worst) to 10 (best) across three four critical dimensions: Instruction Following (instruction adherence), Source Video Preservation (consistency with the source video), Editing Quality (overall video aesthetics), and Subject Similarity (for reference-based edits).



Change the background into ancient castle of Night Magic.



Replace the man into a gorilla.



convert the grayish black car into an armored tank.



Add a dinosaur standing on the ground of gas station.



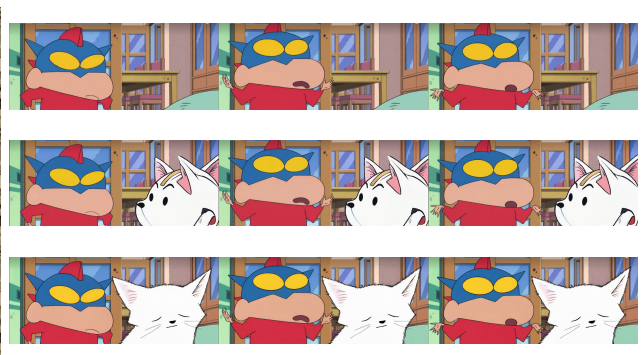
Add a woman with long black hair Lying in the bucket of a green agricultural loader.



Add a big white kitten in the car trunk.



Insert a standing camel with brown fur.



Add a white cartoon cat in the right of the boy.

Figure 10. Ablation studies on Edit-GRPO. Before: without Edit-GRPO; After: with Edit-GRPO. The editing instruction is shown at the bottom.



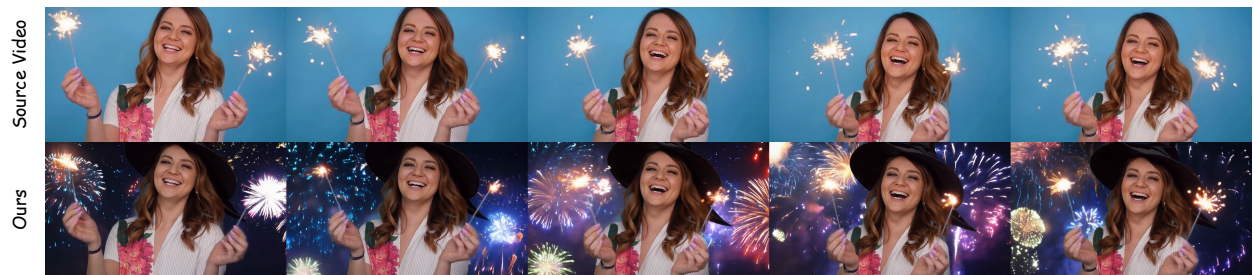
Change the background from the ocean to a vast, snowy mountain range.



Add a trail of fire coming from the back wheel of the bike.



Replace the dumbbells they are holding with flaming torches.



Change the background to a night sky filled with colorful fireworks.



Make the mountain in the background an active volcano erupting with smoke and lava, and add a little cat running by the couple.

Figure 11. Qualitative results. We present more results of our method on complex instructions that are non-trivial and challenging to be synthesized by the data construction pipeline. The editing instruction is shown at the bottom.



Transform the entire scene into oil painting style.



Turn into folded-paper origami art style.



Change the material of the cello to look as if it's carved from a single block of clear ice, and add audience members in the background.



Replace the sky with a swirling, colorful galaxy nebula, and add a panda walking around.



Add a dolphin leaping from the water in the background.

Figure 12. Qualitative results. We present more results of our method on complex instructions that are non-trivial and challenging to be synthesized by the data construction pipeline. The editing instruction is shown at the bottom.



Remove the watermark.



Remove the watermark.



Replace the water in the canal with flowing lava, and add a full head of black hair.



Turn the asphalt road into a vibrant, rainbow-colored path.



Add a pair of large, white, feathered wings to the woman's back, and change woman's hair to red.

Figure 13. Qualitative results. We present more results of our method on complex instructions that are non-trivial and challenging to be synthesized by the data construction pipeline. The editing instruction is shown at the bottom.

<p>**Role:** You are an evaluator for instruction-based video editing tasks. Your job is to assess how well the edited video fulfills the user's specific instructions.</p> <p>**Input** [Input 1: The instruction] [Input 2: The original video] [Input 3: The edited video]</p> <p>**Task:** Please evaluate the instruction-based editing score. Your evaluation should focus on three key aspects: Instruction Following, Edit Quality, and Source Video Preservation.</p> <p>**Scoring Rules**</p> <ol style="list-style-type: none"> 1. Instruction following: Does the edit precisely follow the given instruction? - 7-10: Edit follows the instruction fully. - 4-6: Edit follows the instruction partially. - 0-3: Edit does not follow the instruction. 2. Edit Quality: : Is the edit result video visually seamless and natural-looking? - 7-10: Edit result video is visually seamless fully, natural-looking fully, and aesthetics fully. - 4-6: Edit result video is visually seamless partially, natural-looking partially, and aesthetics partially. - 0-3: Edit result video is not visually seamless, not natural-looking and not aesthetics. 3. Source Video Preservation: Does the edit maintain coherence with the original video context? - 7-10: Edit result video maintains coherence with the original video context fully. - 4-6: Edit result video maintains coherence with the original video context partially. - 0-3: Edit result video does not maintain coherence with the original video context. <p>**Output Rules** Structure the output in JSON format with: - instruction: Repeat the user's instruction. - instruction following score (0-10): [Your score number] - edit quality score (0-10): [Your score number] - source video preservation score (0-10): [Your score number] - reason: The reasons for the score you gave</p> <p style="text-align: center;">Instruction</p>	<p>**Role:** You are an evaluator for instruction-based video editing tasks. Your job is to assess how well the edited video fulfills the user's specific instructions.</p> <p>**Input** [Input 1: The instruction] [Input 2: The original video] [Input 3: The edited video] [Input 4: The reference image]</p> <p>**Task:** Please evaluate the instruction-based editing score. Your evaluation should focus on four key aspects: Instruction Following, Edit Quality, Preservation, and Reference Similarity.</p> <p>**Scoring Rules**</p> <ol style="list-style-type: none"> 1. Instruction following: Does the edit precisely follow the given instruction? - 7-10: Edit follows the instruction fully. - 4-6: Edit follows the instruction partially. - 0-3: Edit does not follow the instruction. 2. Edit Quality: : Is the edit result video visually seamless and natural-looking? - 7-10: Edit result video is visually seamless fully, natural-looking fully, and aesthetics fully. - 4-6: Edit result video is visually seamless partially, natural-looking partially, and aesthetics partially. - 0-3: Edit result video is not visually seamless, not natural-looking and not aesthetics. 3. Source Video Preservation: Does the edit maintain coherence with the original video context? - 7-10: Edit result video maintains coherence with the original video context fully. - 4-6: Edit result video maintains coherence with the original video context partially. - 0-3: Edit result video does not maintain coherence with the original video context. 4. Reference Similarity: Does the edit result video closely match the reference image? - 7-10: Edit result video closely matches the reference image fully. - 4-6: Edit result video closely matches the reference image partially. - 0-3: Edit result video does not closely match the reference image. <p>**Output Rules** Structure the output in JSON format with: - instruction: Repeat the user's instruction. - instruction following score (0-10): [Your score number] - edit quality score (0-10): [Your score number] - source video preservation score (0-10): [Your score number] - similarity to reference_image score (1-10): [Your score number] - reason: The reasons for the score you gave</p> <p style="text-align: center;">Instruction + reference</p>
--	---

Figure 14. VLM templates for the instruction-based video editing and reference-instruction-based video editing.

E. Limitations

Figure 9 presents three failure cases of VIVA. Despite the exceptional generalization capabilities of VIVA, it encounters challenges in specific cases. Rapid motion might occasionally lead to blurry outputs, such as the woman's hand. Furthermore, VIVA sometimes struggles to balance editing intensity: it tends to exhibit over-editing in global transformations (such as weather or style changes) while showing under-editing in removal tasks, where residual artifacts—such as cast shadows—often remain.